FAST TRACK COMMUNICATION

X-ray spectroscopic study of the charge state and local ordering of room-temperature ferromagnetic Mn-doped ZnO

J-H Guo[1,8]**, Amita Gupta**[2]**, Parmanand Sharma**[2,3,7]**, K V Rao**[2]**,
M A Marcus**[1]**, C L Dong**[1,4]**, J M O Guillen**[5]**, S M Butorin**[5]**, M Mattesini**[5]**,
P A Glans**[1,6]**, K E Smith**[6]**, C L Chang**[4]** and R Ahuja**[5]

[1] Advanced Light Source, Lawrence Berkeley National Laboratory, Berkeley, CA 94720, USA
[2] Department of Materials Science, Royal Institute of Technology, SE-100 44 Stockholm, Sweden
[3] Japan Science and Technology Agency, Sendai 980-8577, Japan
[4] Department of Physics, Tamkang University, Tamsui, Taiwan, Republic of China
[5] Department of Physics, Uppsala University, Box 530, SE-751 21 Uppsala, Sweden
[6] Department of Physics, Boston University, 590 Commonwealth Avenue, Boston, MA 02215, USA
[7] Institute for Materials Research, Tohoku University, Sendai 980-8577, Japan

E-mail: jguo@lbl.gov

Abstract
The charge state and local ordering of Mn doped into a pulsed laser deposited single-phase thin film of ZnO are investigated by using x-ray absorption spectroscopy at the O K-edge, Mn K-edge and L-edge, and x-ray emission spectroscopy at the O K-edge and Mn L-edge. This film is ferromagnetic at room temperature. EXAFS measurement shows that Mn^{2+} replaces the Zn site in tetrahedral symmetry, and there is no evidence for either metallic Mn or MnO in the film. Upon Mn doping, the top of O 2p valence band extends into the bandgap, indicating additional charge carriers being created.

Spin-based electronics, using the spin of the electron, is considered to be a promising basis for quantum computing technology as well as non-volatile random access memory (RAM). Independent control of the spin and charge of doped carriers has attracted much interest in diluted magnetic semiconductors (DMSs) [1]. Theoretical calculations predict that Mn-doped p-type ZnO should be ferromagnetic at room temperature [2]. The intensive search in recent years for ferromagnetism above room temperature in DMSs has resulted in the first report of observations of ferromagnetism above room temperature for dilute (<4 at.%) Mn-doped ZnO [3]. The crucial factor in obtaining ferromagnetism above room temperature is that all the sample-processing procedures were carried out at low temperatures (<500 °C). The mechanism

---

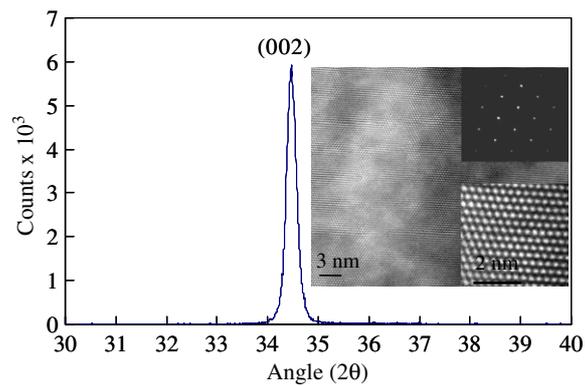[8] Author to whom any correspondence should be addressed.

Figure 1. X-ray diffraction pattern for 2.2 at.% Mn-doped ZnO thin film obtained by pulsed laser ablation, showing that the film is *c*-axis oriented. Inset: high-resolution transmission electron microscope and selected area diffraction pattern, showing that the crystal fragment is oriented perpendicular to the *c*-axis. The measured spacing (0.28 nm) matches the reported {100} lattice spacing for the hexagonal ZnO, and confirmed that the Mn-doped ZnO film used in the present study is free from secondary phases.

(This figure is in colour only in the electronic version)

giving rise to ferromagnetism at such low dopant concentrations was proposed to be the carrier-induced interactions between the separated Mn atoms in ZnO, which has recently been further confirmed beyond doubt by the research group of Gamelin *et al* [4, 5]. Room-temperature ferromagnetism in well-characterized single-phase Mn-doped ZnO has also been reported by many other researchers [4–8]. However, recently, Kundaliya *et al* proposed a different picture, wherein incorporation of Zn in Mn oxide is responsible for ferromagnetism [9]. Such a picture is not in conformity with the study reported by Diaconu *et al* [10] on MnO_2–ZnO compounds. Garcia *et al* [11] showed that the room-temperature ferromagnetism in the Mn–Zn–O system recently observed is associated with the coexistence of Mn^{3+} and Mn^{4+} via a double-exchange mechanism. In view of the continued controversy over reports of process-dependent results on Mn-doped ZnO (ZnO:Mn), varying from non-magnets to homogeneous ferromagnets, in this work we present extensive in-depth extended x-ray absorption edge fine structure (EXAFS), x-ray absorption spectroscopy (XAS) and x-ray emission spectroscopy (XES) electronic structure studies on the same high-quality single-phase pulsed laser deposited film reported by Sharma *et al* [3]. Such studies have been found to be consistent on more than one thin film of ZnO:Mn.

EXAFS reveals the local structure change upon Mn doping in ZnO lattices, and L-edge XAS and XES studies give insight into the possible existence of strong p–d hybridization in ZnO:Mn and also offer an alternative method for determining the bandgap [12, 13]. In Co-doped ZnO, several experiments have suggested a strong p–d exchange interaction and ferromagnetic behaviour [14, 15]. So far, rather few x-ray spectroscopic studies on Mn-doped ZnO have been reported [16]. There is no information on how Mn doping induces changes in the electronic structure of the host ZnO lattices. In this letter we discuss for the first time the electronic properties, from XAS and XES studies, of the same well-characterized homogeneous thin-film pulsed laser deposited room-temperature ferromagnets, as reported by Sharma *et al* [3, 17].

The ZnO:Mn thin film was deposited on a fused quartz substrate by a pulsed laser ablation (PLA) technique, as described in [3]. The Mn concentration is about 2.2 at.%. X-ray diffraction (XRD), high-resolution TEM, selected area diffraction patterns (figure 1), and energy dispersive
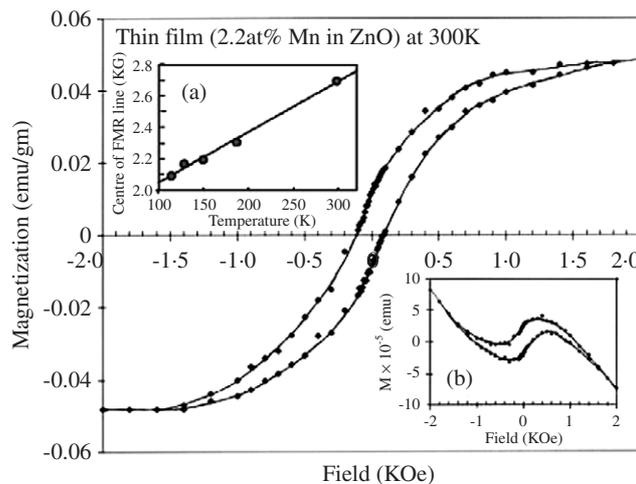
IOP FTC ▶▶▶

J. Phys.: Condens. Matter **19** (2007) 172202   Fast Track Communication

Figure 2. Magnetization at 300 K for 2.2 at.% Mn-doped ZnO thin film. The curve was obtained after subtracting the diamagnetic contribution from the substrate. Insets: (a) temperature dependence of the position of the centre of the ferromagnetic resonance (FMR) line—fitting it to a straight line and extrapolating to the temperature where the position would be the same as the paramagnetic line gives the T_c above ∼400 K; (b) As-obtained $M(H)$ curve from the SQUID measurements along with the diamagnetic contribution arising from the fused quartz substrate.

and electron energy loss spectroscopic measurements confirmed the *c*-axis oriented growth free from secondary phases, with the Mn homogeneously distributed and divalent [3]. Magnetic characterization with ferromagnetic resonance and a superconducting quantum interference device (SQUID) magnetometer (figure 2) revealed that the pulsed laser deposited Mn-doped ZnO thin films are ferromagnetic, with a T_c above ∼400 K [17]. The detailed structural and magnetic characterization of the ZnO:Mn thin films used in the present study can be found in the references [3] and [17]. We must point out that such films are now produced routinely in our group. We have also obtained above-room-temperature transparent ferromagnetic thin films of ZnO:Mn deposited by RF/dc magnetron sputtering on fused quartz substrate.

The x-ray spectroscopic experiments to probe the electronic structure of ZnO single crystal and Mn-doped ZnO single-phase thin film were performed on BL7.0 at the Advanced Light Source [18]. The XAS spectra were obtained by measuring the fluorescence yield and photocurrent from the sample with a resolution of 0.15 and 0.2 eV for O K-edge and Mn L-edge absorption, respectively. The resolution of the incident-beam monochromator was 0.5 eV for the XES measurements. The XES spectra were recorded using a grating spectrometer [19] with a resolution of 0.4 and 0.6 eV for O K- and Mn L-emissions, respectively. The incidence angle was 30° to the sample surface to minimize the self-absorption effect in XES measurements. Mn K-edge EXAFS measurements were performed at ALS BL10.3.2 [20] in grazing incidence. The data were analysed with reference to spectra from pure ZnO and calculations with FEFF8.1 [21].

Figure 3 shows the Fourier transforms of the ZnO:Mn and pure ZnO data, compared with FEFF two-shell fits. The fit shows a first-shell coordination for Mn of 3±0.5 O at 2.054±0.02 Å (ZnO: 4@1.98 Å) and a second-shell coordination of 11 ± 3 Zn at 2.24 ± 0.02 Å (ZnO: 12@2.23 Å, ignoring the 1 O sitting among the second neighbours). The Fourier transform (FT) immediately suggests a similarity of environment between Mn and Zn in ZnO, which is borne out by the fits. The expansion of the first shell around the Mn is reasonable given that
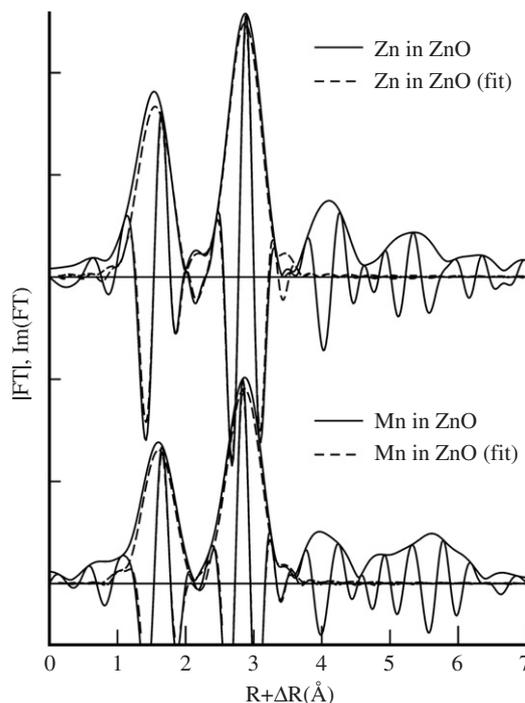
3

IOP FTC ▶▶▶

J. Phys.: Condens. Matter **19** (2007) 172202   Fast Track Communication

Figure 3. Comparison of EXAFS Fourier transforms for pure ZnO (upper) curves and Mn in ZnO (lower). The dashed lines show the two-shell FEFF fits.

the Mn^{2+} ion is larger than the Zn^{2+} ion it replaces (ionic radii of 0.91 Å versus 0.82 Å). The mean-square relative displacement (second moment of the distance distribution) does not differ detectably between Mn and Zn, suggesting that the Mn is on-centre or nearly so. The spectra do not resemble those of any Mn oxide or metallic Mn.

The Mn L-edge XAS spectrum of ZnO:Mn is shown in figure 4(a). The absorption features in the region of 640–648 eV with a main absorption peak at 642.5 eV are assigned to the Mn $2p_{3/2}-3d$ (L_3 edge) transitions, and those in the region of 652–657 eV to the Mn $2p_{1/2}-3d$ (L_2 edge) transitions. The Mn 2p absorption has been shown to be highly sensitive to the local symmetry of the Mn sites and their formal valency [22, 23]. The x-ray absorption spectra show a shift to higher energy for the main L_3-edge absorption features as the charge states change from Mn^{2+}, Mn^{3+} and Mn^{4+}, and the spectral shape changes significantly with the number of 3d electrons. Thus, the separation and intensity distribution of absorption peaks A_1-A_3 (figure 4(a)) make determination of the charge state and crystal-field splitting straightforward. The Mn L-edge absorption spectrum of ZnO:Mn is similar to that of MnO [24], which also suggests the charge state of Mn^{2+}.

The Mn L-edge emission spectrum, which is originated from the transitions of Mn 3d to 2p states, is shown in figure 4(b). The energy separation between emission lines β_1 and β_2 is 11.1 eV and comes from the spin orbital splitting of $2p_{1/2}$ and $2p_{3/2}$, while emission lines β'_1 and β_2 are only 8 eV apart. The Mn L-edge emission lines are reflections of Mn occupied 3d states. The strong emission line β'_1 was not observed in MnO [24], which suggests that the Mn^{2+} has a chemical environment of a ZnO matrix rather than a MnO local structure.

In order to determine the effect of Mn doping on the electronic structure of ZnO:Mn, we turn to the O K-edge for the detailed analysis. The O K-edge absorption and emission spectra
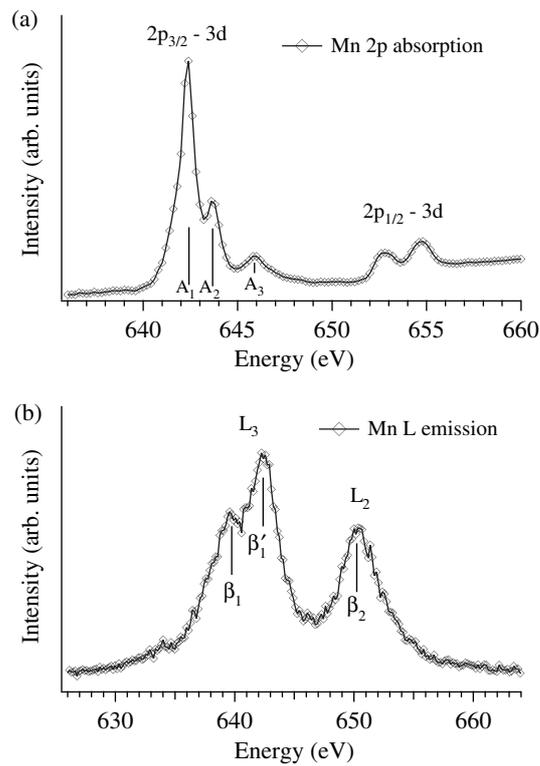
Figure 4. Mn L-edge absorption spectrum of ZnO:Mn (a) and Mn L-emission spectrum of ZnO:Mn (b).
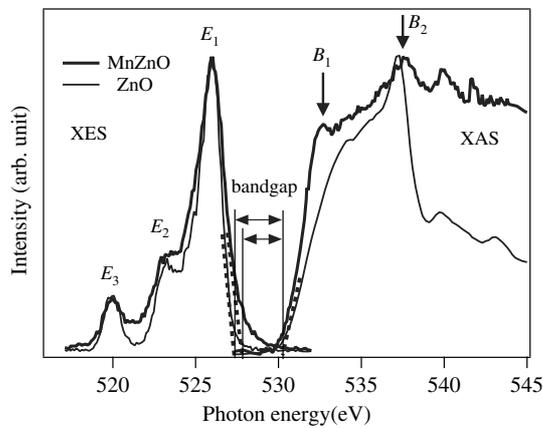

Figure 5. Oxygen x-ray *absorption–emission* spectrum reflecting conduction and valence bands of ZnO and ZnO:Mn.

of ZnO and ZnO:Mn are displayed in figure 5. The O K-emission spectrum reflects the O 2p valence band, and the O K-edge absorption spectrum the O 2p conduction band. The valence-band maximum and the conduction-band minimum are separated by about 3.2 eV for ZnO, and reduced to about 2.9 eV for ZnO:Mn. Such a change is seen mostly to be due to the appearance

IOP FTC ▶▶▶

J. Phys.: Condens. Matter **19** (2007) 172202   Fast Track Communication

of the new states close to the top of the valence band induced by Mn doping, although there is an intensity enhancement in the region of a few eV above the pre-edge of the XAS spectrum of ZnO:Mn. It is well known that the absorption intensities in the pre-edge region of 530–535 eV result from the hybridization of O 2p and metal 3d states, and the absorption intensity in this region has become a measure of the hybridization strength of these materials [25]. The smaller intensity of absorption feature in this region of the O K-edge absorption spectrum for undoped ZnO indicates that there is very little mixing between Zn 3d and O 2p states in the conduction band [12]. Therefore, the increased intensity of pre-edge features in the O K-edge absorption spectrum of ZnO:Mn (around the arrow B_1 in figure 5) is attributed to the hybridization between Mn 3d and O 2p states upon Mn doping. Also, there may be an involvement of Zn 4s states too.

O K-emission spectra of both pure and Mn-doped ZnO show three distinct structures labelled E_1, E_2, and E_3. For ZnO, feature E_1, located at ∼526 eV, is mainly due to O 2p– Zn 4p states [13]. The low-energy shoulder (feature E_2) in the 522–524 eV region arises from the mixed states of O 2p–Zn 4s. The single-band shape (E_3) at 520 eV is attributed mainly to the O 2p hybridized with Zn 3d states. All three-emission bands become broader upon Mn doping. The top of valence band shows a sharp intensity decay in the case of ZnO compared to ZnO:Mn, which pushes the valence band maximum edge into the bandgap.

The increased weight at the top of the valence band of ZnO:Mn is attributed to Mn doping into ZnO. The O K-edge absorption and emission suggest that the electronic properties of the doped thin film are rather close to those of ZnO, with additional charge carriers originating from Mn doping [3]. As Mn^{2+} substitutes for Zn^{2+} in the ZnO matrix, there is no need for oxygen vacancies for charge compensation, as no shift is observed at the bottom of the conduction band (XAS spectrum). The new states appearing at the top of the valence band (XES spectrum) in Mn-doped ZnO suggests that Mn doping induces charge carriers in ZnO. The experimental findings suggest that the ferromagnetism in ZnO:Mn may be charge-carrier induced, in contrast to other room-temperature ferromagnetic semiconductors such as Co-doped TiO_2, in which an oxygen vacancy is found [26]. Also, the involvement of Zn 4s states may lead to ferromagnetic ordering.

In conclusion, the charge state and local structure of Mn doped in ZnO have been investigated by using various experimental techniques. XRD, EXAFS, and Mn L-edge absorption studies indicate that Mn^{2+} substitutes for Zn in tetrahedral symmetry. The O 2p absorption and K emission spectra reveal a strong hybridization between Mn 3d and O 2p. The electronic structure of ZnO:Mn is rather close to that of undoped ZnO, with additional charge carriers from Mn doping. The mechanism of above-room-temperature ferromagnetism in ZnO:Mn may be due to the carrier-induced interaction between the Mn atoms in ZnO.

References

[1] Ohno H 1998 *Science* **281** 951
      Ohno Y *et al* 1999 *Nature* **407** 790
      Beschoten B *et al* 1999 *Phys. Rev. Lett.* **83** 3073
[2] Dietl T, Ohno H, Matsukura F, Cibert J and Ferrand D 2000 *Science* **287** 1019

[3]   Sharma P, Gupta A, Rao K V, Owens F J, Sharma R, Ahuja R, Osorio Guillen J M, Johannson B and
        Gehring G A 2003 *Nat. Mater.* **2** 673
[4]   Norberg N S, Kittilstved K R, Amonette J E, Kukkadapu R K, Schwartz D A and Gamelin D R 2004 *J. Am.
        Chem. Soc.* **126** 9387
[5]   Kittilstved K R, Norberg N S and Gamelin D R 2005 *Phys. Rev. Lett.* **94** 147209
[6]   Heo Y W, Ivill M P, Ip K, Norton D P, Pearton S J, Kelly J G, Rairigh R, Hebard A F and Steiner T 2004 *Appl.
        Phys. Lett.* **84** 2292
[7]   Blythe H J, Ibrahim R M, Gehring G A, Neal J R and Fox A M 2004 *J. Magn. Magn. Mater.* **283** 117
[8]   Pradhan A K *et al* 2005 *Appl. Phys. Lett.* **86** 152511
[9]   Darshan C *et al* 2004 *Nat. Mater.* **3** 709
[10] Diaconu M, Schmidt H, Pöppl A, Böttcher R, Hoentsch J, Klunker A, Spemann D, Hochmuth H, Lorenz M and
        Grundmann M 2005 *Phys. Rev.* B **72** 85214
[11] Garcia M A *et al* 2005 *Phys. Rev. Lett.* **94** 217206
[12] Guo J-H, Vayssieres L, Persson C, Ahuja R, Johansson B and Nordgren J 2002 *J. Phys.: Condens. Matter*
        14 6969
[13] Dong C L, Persson C, Vayssieres L, Augustsson A, Schmitt T, Mattesini M, Ahuja R, Chang C L and
        Guo J-H 2004 *Phys. Rev.* B **70** 195325
[14] Kim K J and Park Y R 2002 *Appl. Phys. Lett.* **81** 1420
        Ando K, Saito H, Jin Z, Fukumura T, Kawasaki M, Matsumoto Y and Koinuma H 2001 *Appl. Phys. Lett.* **78** 2700
[15] Ueda K, Tabata H and Kawai M 2001 *Appl. Phys. Lett.* **79** 988
        Lee H-J, Jeong S-Y, Cho C R and Park C H 2002 *Appl. Phys. Lett.* **81** 4020
[16] Okabayashi J *et al* 2004 *J. Appl. Phys.* **95** 3573
[17] Sharma P, Gupta A, Owens F J, Inoue A and Rao K V 2004 *J. Magn. Magn. Mater.* **282** 115
[18] Warwick T, Heimann P, Mossessian D, McKinney W and Padmore H 1995 *Rev. Sci. Instrum.* **66** 2037
[19] Nordgren J, Bray G, Cramm S, Nyholm R, Rubensson J-E and Wassdahl N 1989 *Rev. Sci. Instrum.* **60** 1690
[20] Marcus M A, MacDowell A A, Celestre R, Manceau A, Miller T, Padmore H A and Sublett R E 2004
        J. Synchrotron Radiat. **11** 239
[21] Ankudinov A L, Ravel B, Rehr J J and Conradson S D 1998 *Phys. Rev.* B **58** 7565
[22] de Groot F M F, Fuggle J C, Thole B T and Sawatzky G A 1990 *Phys. Rev.* B **42** 5459
[23] van der Laan G and Kirkman I W 1992 *J. Phys.: Condens. Matter* **4** 4189
[24] Butorin S M, Guo J-H, Magnuson M, Kuiper P and Nordgren J 1996 *Phys. Rev.* B **54** 4405
        Butorin S M 2000 *J. Electron. Spectrosc. Relat. Phenom.* **110/111** 213
[25] de Groot F M F, Grioni M, Fuggle J C, Ghijsen J, Sawatzky G A and Petersen H 1989 *Phys. Rev.* B **40** 5715
[26] Chambers S A, Heald S M and Droubay T 2003 *Phys. Rev.* B **67** 100401